Computational Approaches for the Programmed Assembly of Nanocellulose Meshes

Alexandru Amarioarei[1], Frankie Spencer[2], Corina Itscus[1], Iris Tusa[1], Ana-Maria Dobre[1], Gefry Barad[1], Romica Trandafir[1], Mihaela Paun[1], Andrei Paun[1], and Eugen Czeizler[1,2]

[1] Nat. Ins. of Research and Development for Biological Sciences, Bucharest, Romania
[2] Department of Computer Science, Åbo Akademi University, Turku, Finland

Nanoengineered materials are a product of joint collaboration of theoreticians and experimentalists, of physicists, (bio-)chemists, and recently, of computer scientists. In the field of Nanotechnology and Nanoengineering, DNA (algorithmic) self-assembly has an acknowledged leading position. As a fabric, DNA is a rather inferior material; as a medium for shape, pattern, and dynamic behavior reconstruction, it is one of the most versatile nanomaterials. This is why the prospect of combining the physical properties of known high performance nanomaterials, such as cellulose, graphene, or fibroin, with the assembly functionality of DNA scaffolds is a very promising prospect. In this research we analyze the dynamical and structural properties of a would-be DNA-guided assembly of nanocellulose meshes. The aim is to generate pre-experimental insights on possible ways of manipulating structural properties of such meshes. The mechanistic principles of these systems, implemented through the DNA assembly apparatus, ensure the formation of 2D nanocellulose mesh structures. A key desired feature for such an engineered synthetic material, e.g. with applications in bio-medicine and nanoengineering, would be to control the size of the openings (gaps) within these meshes, aka its aperture. However, in the case of this composite material, this is not a direct engineered feature. Rather, we assert it could be indirectly achieved through varying several key parameters of the system. We consider here several experimentally tunable parameters, such as the ratio between nanocellulose fibrils and the DNA guiding elements, i.e., aptamer-functionalized DNA origamis, as well as the assumed length of the nanocellulose fibrils. For that we create a computational model of the mesh-assembly dynamical system, which we subject to parameter scan and numerical analysis.

In this research we want to capture and analyze the guided assembly of nanocellulose rods (R) with the help of DNA-based macro-structures (O), i.e., DNA origamis, which are functionalized with cellulose binding DNA aptamers and are acting as a smart-ligand in between two rods. Moreover, using precise sequence matchings and positioning of the aptamers, one can hope of obtaining a perfect orthogonal positioning of each two intersecting rods, as exemplified in Fig. 1. While experimental implementations of such systems are currently on incipient stages in our laboratories, in this research we analyze the possibility of controlling the average aperture of these meshes, i.e., the average fully surrounded openings

within the mesh, by varying a series of experimentally attainable parameters, such as the O/R ratio of initial reactants and the length l of the rods[3].

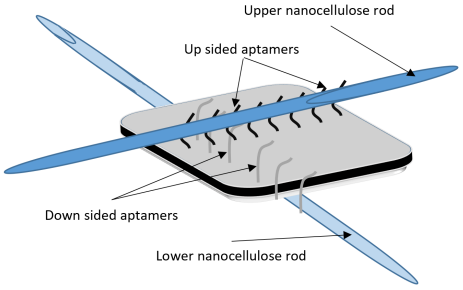

Fig. 1. DNA origami functionalized by orthogonally aligned cellulose aptamers, placed on opposite sides, and connected to nanocellulose fibrils

A somewhat simplified discrete dynamical model of the above process can be described as follows: The rods (R) are fixed length objects, with a fixed maximal number l of consecutive docking positions. These docking positions can be occupied only by square 2-dimensional DNA origami (O) constructs. Each O can connect to exactly two Rs, each of them on one of the sides of these structures, such that the two Rs will be placed on orthogonal position, as in Fig. 1. Thus, once an origami is docked on one rod's docking position, another rod can dock on this origami, thus enlarging the assembly; in this study we assume that the R-O binding interactions are irreversible. By subsequent assemblies of rod and origami elements, the rods will ultimately assemble into a patchy mesh structure, where the holes of this structure will vary depending on the values of several parameters. As in previous study of self-assembly systems, we will assume that only elementary structures, i.e., R and O, can attach to an assembly, and that partial assemblies are not interacting with one another[4]. The parameters identified by us as both significant and experimentally achievable in order to influence the average aperture size of the final assembled meshes are the ratio between the number of rods and origamis in the system, $s = O/R$, and the discrete length l of these rods.

Results

Our analysis of the cellulose-mesh dynamical system is based on a coarse-grained modeling methodology performed using the agent- and rule-based modeling

[3] While in reality we expect the length of these rods to be variable, for simplification reasons in this study we assume a uniform length for these elements, which could be considered e.g. as the average length

[4] While we acknowledge that some partial assemblies might interact with one-another, at this moment it is not clear for us if a stability/binding-strength threshold should be added in order to enable such merger, as well as how -or if- such interactions can be captured in our computational model

framework of the BioNetGen language (BNGL) [1], while the associated numerical integration is performed with the NFsim [3] and RuleBender [2] software tools. Although BNGL is by default a coarse grained modeling methodology, and thus will capture the exact structural complexness of the emerging assembly, its output is restricted to pre-defined user queries. For example, we could interrogate the system about the number of R (or O) objects within the assembly at some time point, or the number of O which are connected only to one R, etc. ,but we can not, by default, list the entire emerging assembly structure. On the other hand, NFsim allows the creation of dump files at specific (model) time points, from which we can reconstruct the entire state of the system, incl. the structure of the emerging assembly, at that time point. Thus, we have created specific Python subroutines for parsing the model dump file at specific timepoints, and extract the structural arrangement of the rods within the current state of the emerging assembly. This structural arrangement is then represented as a 2D integer matrix, whose entry on point (i, j) has value k, $k \geq 0$, iff there are exactly k superimposed R objects on the (discrete) position (i, j). We use this matrix representation of the assembly in order to analyze the average distribution of inter-rod spaces, a.k.a. the average mesh gaps. Moreover, since the size of these gaps is bound to be influenced by their relative position within the mesh, i.e., central locations are expected to exhibit smaller gap size, we can further provide a localized statistics of the average gap size, based on a user-defined zoning granulation of the mesh. By default, in our analysis we have used a 4×4 partitioning of the structures. During successive in-silico experiments we span the $s = O/R$ ratio through the values 0.1, 0.5, 1, 5, and 10, respectively, while l is spanned through the values 5, 10, 15, and 20, respectively. In all our experiments we keep fixed the concentration of free-floating R objects, $|R| = 1000$, and we numerically simulate each of these scenarios up to the point where the number of rods captured within the mesh reaches 1000.

Data analysis of the results is performed by tracking the mean aperture of the holes in the mesh, computed both over the entire structure, and over the 4×4 partitions (in total 1+16 mean values). We repeat each experiment 9 times and we record the median values both per the entire structure, see Fig. 2 and column *str* in Table 1 (displayed in the Appendix), and per each of the 16 zones independently, see columns $zn\ k, 1 \leq k \leq 16$, in Table 1. When analyzing the data we defined the surface of the assembled structure as the area between the coordinates of the top and bottom horizontal R, and the left-most and right-most vertical R, and for positioning of the individual gaps within the structure we have used their center of mass.

From the reported data we can conclude that enlarging the overall length of the rods does indeed generate explicit and measurable differences in the size of the mesh openings. This is particularly encouraging, as it gives a clear indication of the possibility of being able to engineer nanocellulose meshes with custom-build average apertures. Also, it turns out that varying the O/R ratio, even among two orders of magnitude, generates a much softer response in terms of the average gap sizes. However, this parameter does indeed have a significant

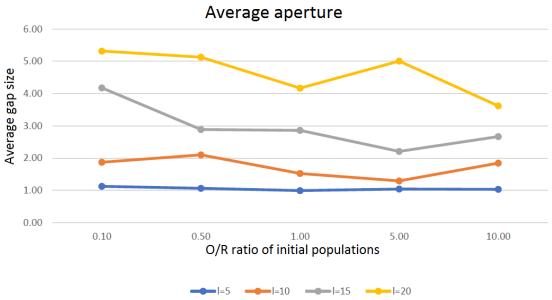

Fig. 2. Dynamics of the assembly-averaged gap size per O/R and rod length variation. Each data point is a median of 9 independent runs. The horizontal axes represents the O/R parameter and the vertical one is the average size of the hole. All assemblies contain 1000 rods.

contribution to the speed of the system, as we observed a linear correlation between these two features (data not shown). Another interesting observation is that neither of the two parameters, i.e., the length of the rods and the O/R ratio, seem to have a significant leverage over the holes distribution along the surface of the mesh, see e.g. the average gap distribution from Table 1. This makes us question whether we can find yet another parameter which could be used to influence also this feature of the system.

References

[1] James R. Faeder, Michael L. Blinov, Byron Goldstein, William, and S. Hlavacek. Rule-based modeling of biochemical networks. *Complexity*, 10:22–41, 2005.

[2] A.M. Smith, W. Xu, Y. Sun, J.R. Faeder, and G.E. Marai. Rulebender: Integrated modeling, simulation and visualization for rule-based intracellular biochemistry. *BMC Journal of Bioinformatics*, 13:1–16, Jun 2012.

[3] M. Sneddon, J. Faeder, and T. Emonet. Efficient modeling, simulation and coarse-graining of biological complexity with nfsim. *Nature methods*, 8(2):177–183, 2011.

Appendix

R/O	Average hole size																
	zn 1	zn 2	zn 3	zn 4	zn 5	zn 6	zn 7	zn 8	zn 9	zn 10	zn 11	zn 12	zn 13	zn 14	zn 15	zn 16	str
0.10	0	2,2	1,4	0	1,17	1,0	1,06	1,38	1,78	1	1,06	1,25	1	1,43	1,25	1	1,13
0,50	0	2,14	1,38	0	1,19	1,04	1	1,25	1,15	1	1	1,5	2	1,25	1,13	0	1,06
1,00	0	1,4	1,67	0	1,57	1	1	1,63	1,4	1	1	1,6	0	1,55	1,11	0	1,00
5,00	0	1,12	1,27	1	1,15	1	1	1	1	1	1	1,31	0	1,24	1,58	2	1,04
10,00	1	1,22	1,46	1	1,13	1	1	1,22	1,67	1	1	1,19	0	1,44	1,22	0	1,03

a) Rod length $l = 5$

R/O	Average hole size																
	zn 1	zn 2	zn 3	zn 4	zn 5	zn 6	zn 7	zn 8	zn 9	zn 10	zn 11	zn 12	zn 13	zn 14	zn 15	zn 16	str
0,10	0	4	3,86	0	2,48	1,48	1,01	2,29	2,43	1,13	1,03	2	0	3	2,45	2,86	1,88
0,50	0	4,14	3	0	4,14	1,38	1,11	4,73	3,71	1,04	1,12	2,64	1,91	1,79	2,94	0	2,10
1,00	0	2,44	2,5	0	2,76	1,05	1,11	3	2,17	1,05	1,2	2,07	0	2,25	2,84	0	1,53
5,00	0	1,57	1,59	0	2,33	1,21	1,04	1,74	2,5	1,09	1,02	1,94	0	2,3	2,4	0	1,30
10,00	0	2,21	4	0	1,89	1,09	1,18	1,6	3,89	1,19	1,03	1,36	0	5,07	2,07	3	1,85

b) Rod length $l = 10$

R/O	Average hole size																
	zn 1	zn 2	zn 3	zn 4	zn 5	zn 6	zn 7	zn 8	zn 9	zn 10	zn 11	zn 12	zn 13	zn 14	zn 15	zn 16	str
0,10	0	6,05	6,02	13,17	4	1,52	1,32	4,48	8,77	1,96	1,67	4,6	0	5,93	7,36	0	4,18
0,50	0	3,48	4,66	0	4,13	1,2	1,24	7,26	5,33	1,36	1,65	4,37	0	5,13	6,43	0	2,89
1,00	0	2,3	6,53	0	4,41	1,51	1,77	7	4,43	1,15	1,54	5,17	0	5,67	4,32	0	2,86
5,00	0	4,71	5,65	0	2,96	1,2	1,17	2,29	4,33	1,33	1,11	3,46	0	4,43	2,64	0	2,21
10,00	0	9,26	2,75	0	4,54	1,61	1,35	4,19	4,82	1,26	1,28	3,65	1,67	3,52	2,8	0	2,67

c) Rod length $l = 15$

R/O	Average hole size																
	zn 1	zn 2	zn 3	zn 4	zn 5	zn 6	zn 7	zn 8	zn 9	zn 10	zn 11	zn 12	zn 13	zn 14	zn 15	zn 16	str
0,10	0	6,78	9,87	0	9	1,57	1,88	8,87	8,5	1,75	1,73	13,4	0	11	10,74	0	5,32
0,50	0	18,06	7,61	0	7,2	1,7	1,77	5,19	8,39	1,62	1,65	9,56	5,46	6,33	7,6	0	5,13
1,00	0	6,15	10	0	5,42	1,63	1,53	6,88	4,5	1,56	1,58	8,79	5	8,6	5,12	0	4,17
5,00	0	7,55	8,92	0	6,17	1,51	1,51	6,74	10,6	1,32	1,64	7,38	14,33	4,89	7,64	0	5,01
10,00	0	6,33	5,1	0	5	1,45	1,38	5,04	8,15	1,69	1,47	8,53	0	7,43	6,42	0	3,62

d) Rod length $l = 20$

Table 1. Evolution of the average gap size per O/R ratio variation, when the rod length l, i.e., the max. number of consecutive origami docking positions, is a) 5, b) 10, c) 15, and d) 20. The table entries represent mean apertures of the holes in the mesh, by averaging both over a 4×4 zoning of the structure (with zone 1 and zone 4 on the top left and right corner, and zone 13 and zone 16 on the bottom left and right corners, respectively), as well as over the entire assembly. Each entry is the median of 9 independent runs of the in-silico experiments, performed with the same O/R and l parameter valuations.